

An assessment of the magmatic conditions of Dinh Quan – Deo Ca – Ankoet granitoids: evaluating from the igneous rocks at SW Vietnam - SE Cambodia

Thuy Thanh PHAM^{1,2*}

¹ Faculty of Geology, University of Science, Ho Chi Minh City, Vietnam.

² Vietnam National University, Ho Chi Minh City, Vietnam.

* Corresponding email: pththuy@hcmus.edu.vn

Abstract: *The Dinh Quan – Deo Ca – Ankoet granitoids in SW Vietnam-SE Cambodia occur in small bodies of Late Mesozoic igneous rocks, including Bay Nui-Ba Den (BN-BD) diorite (107 – 96 Ma), Bach Ho (BH) granitoid (110 Ma), Bay Nui-Phnom Den (BN-PD) granitoid (94 – 91 Ma); Con Dao (CD) suite (83 Ma), Pha Aok (PA) (78 Ma), and Nui Sam-Angkor Borei (NS-AB) granitoid suite (75 Ma). These granitoids correspond to two tectonic stages: (I) Paleo-Pacific subduction (110 – 90 Ma) and (II) transitional crust extension phase (83 – 75 Ma) which is prior to the sea-opening in Cenozoic. This study utilizes biotite composition as a geobarometer to estimate the magmatic conditions (P, T) of these granitoids. The Al-in-biotite method estimates magmatic conditions for I-type granitic rocks at P = 0.097 – 0.117 GPa, T = 749 – 761°C (BN-BD); P = 0.031 – 0.096 GPa, T = 628 – 759°C (BN-PD); and P = 0.262 – 0.272 GPa, T = 642°C (BH). A-type granites are characterized by P = 0.081 GPa, T = 885°C (CD), P = 0.311 – 0.408 GPa, T = 605 – 626°C (PA), and P = 0.292 – 0.316 GPa, T = 603 – 608°C (NS-AB). The classification of NS-AB and PA granites, previously identified as A-type, shows characteristics aligning with peraluminous, highly contaminated, and reduced I-type granites. Rhyolite MELTs modeling supports these findings, indicating I-type granitoids crystallized at P = 0.3 GPa and T = 1005–730°C under reduced oxygen conditions ($\Delta FMQ -1$), except for BH, which shows a more oxidized state ($\Delta FMQ +1$). A-type/SCR I-type granites formed at P = 0.35–0.4 GPa and T = 1105–758°C under reduced conditions ($\Delta FMQ -3$ to -1). The Paleo-Pacific subduction-related granites formed at shallower depths, whereas the extensional related granitoids crystallized at greater depths with distinct redox conditions. These findings provide crucial insights into magmatic evolution and regional tectonics.*

Keywords: *Dinh Quan – Deo Ca – Ankoet granitoids; magmatic conditions; pressure; depth; temperature; fugacity oxygen; relatively oxidized; reduced*

1. Introduction

During the Late Mesozoic (110 to 90 Ma), the tectonic and magmatic evolution of Southeast Asia, particularly in southwest Vietnam and southeast Cambodia, was profoundly affected by the subduction of the Paleo-Pacific beneath the Eurasian. This convergence triggered extensive volcanic activities and led to the formation of diverse granitoid complexes. In southwest Vietnam and southeast Cambodia, typically the Indochina Block, the Dinh Quan - Deo Ca and Ankoet granitic complexes, represent significant Late Mesozoic magmatism activities [1] [2] [3] [4]. These granitoids mainly extends in the Dalat Zone [5] and some igneous suites in SW Vietnam and SE Cambodia [6]. These are Bay Nui-Ba Den (BN-BD) diorite (107 – 96 Ma), Bach Ho (BH) I-type granite suite (110 Ma), Bay Nui-Phnom Den (BN-PD) I-type granite suite (94 – 91 Ma); Con Dao (CD) A-type granite suite (83 Ma), Pha Aok (PA) (78 Ma) A-type granite suite, and Nui Sam-Angkor Borei (NS-AB) A-type granite suite (75 Ma). These petrogeneses of those two granitic types may related to two tectonic events: (I) Paleo-Pacific subduction (110 – 90 Ma) and (II) transitional crust extension phase (83 – 75 Ma) which is prior to the sea-opening in Cenozoic (Nong et al., 2021 - [6]).

Biotite, a mafic mineral, plays crucial role in granitic rocks. It's compositions offer insights into magmatic conditions and the nature of the parental magma during crystallization [7] [8]. Studying the biotite composition can serve multiple purposes: (1) tracking the oxidation state of the melt [9] [10] [11], (2) discriminating geotectonic settings [12] [7] [8], (3) estimating crystallization temperature [13], and (4) constraining the depth of crystallization [14]. Rhyolite MELTS model is a set of computational tools used in igneous petrology and volcanology. These models can be used to simulate the crystallization and differentiation processes of felsic magmas. The mineral assemblages, phase equilibria, and geochemical signatures associated with rhyolitic/granitic formation can be predicted by inputting parameters such as temperature, pressure, and melt composition. The Rhyolite MELTS model is utilized to understand volcanic eruptions, magma evolution, and the dynamics of Earth's crust. Its applications extend to unraveling the complexities of magmatic systems and interpreting geological records [15].

In regard to the vital roles of the Dinh Quan - Deo Ca - Ankoet granitic complexes, the petrology and genesis have been extensively studied in previous publications [1] [2] [3] [16] [17] [6], the magmatic conditions crucial for elucidating the tectonomagmatic environment have received comparatively limited attention; except the work of [6]. [6] reported the geochemistry of olivine, amphibole, biotite, pyroxene, and feldspar, and then estimated the crystallization pressure, temperature, and redox conditions using various geobarometers and thermometers. The Al-in-hornblende barometer [18] has been applied to indicate pressures of 0.2 – 0.37 GPa for the BN-BD diorite, 0.3 – 0.39 GPa for the BH granodiorite, and 0.24 – 0.32 GPa for the CD granites. [6] used the empirical after [19] to estimate the pressure for amphibole-free granitic rocks and reported a 0.13 – 0.22 GPa for the BN-PD granitoids, 0.19 – 0.22 GPa for the PA rocks, and 0.11 – 0.14 GPa for the NS-AB rocks. Zircon saturation thermometry yielded temperatures of 750 – 790°C for the BN-BD diorite, 735 – 837°C for the BN-PD granitoids, and 855 – 875°C for the CD granites. The BN-BD and BH suites exhibited oxidized conditions, while the PA and NS-AB suites were more reduced, characterized by ilmenite dominance [6].

This research conducted a re-calculation of biotite chemistry in I-type and A-type granites sourced from the Dinh Quan – Deo Ca – Ankoets region, building upon the findings of [6]. The aims of the research is to include detailing the mineral-chemical progression of the “Primary magmatic biotite”, the biotite grain that has not been altered by the hydrothermal or the circulation of various late- to post-magmatic fluids [12], within these granites, assessing the magmatic parameters (such as pressure, crystallization temperature, and oxygen fugacity) during biotite formation, identifying geochemical variations in biotite and exploring the tectono-magmatic consequences. Furthermore, the Rhyolite MELTs software are utilized to create crystallization models based on previously reported bulk-rock compositions [6], facilitating the calculation of magmatic conditions and allowing for a comparison with mineral chemistry data. The results enhance the understanding of the long-term evolution of magmatism as it shifts from a subduction-related environment to one characterized by post-subduction extension, thereby offering additional insights into crustal development processes in the southwestern region of Vietnam and southeastern region of Cambodia.

2. Geological background

The study area covers approximately 100,000 km² within the southern Indochina Block, located on the southeastern margin of Sundaland (Fig. 1). This region, composed of remnants from the Tethys Ocean and fragments of Gondwana, is positioned near active subduction zones at the convergence of major tectonic plates [20] [21]. The amalgamation of the Indochina and South China blocks during the Late Paleozoic to Early Mesozoic resulted in the formation of a Mesozoic igneous belt. The Dalat zone, characterized by the Dinh Quan – Deo Ca – Ankoet igneous suites, represents a typical convergent margin and is part of a Late Mesozoic intrusive belt extending from Japan to southwestern Borneo [22] [17]. It is separated from the Dalat zone by the Oligocene Wang Chao fault [23]. The termination of Paleo-Pacific subduction is attributed to slab retreat or the collision between the Indochina and Luconia blocks [17]. Cenozoic rifting and basaltic volcanism were prominent in south-central Vietnam [24]. The oldest rocks in the Indochina block are Paleo- to Mesoproterozoic metamorphic formations around Kontum, overlain by marine deposits from the Paleozoic to Triassic and Jurassic-Cretaceous periods.

The Dinh Quan-Deo Ca granitoid complexes ($\gamma\delta K_1 d\bar{d}$) include diorite, granodiorite, and granite, primarily found in Central and southern Vietnam, particularly within the Da Lat structure. These rocks are rich in quartz, plagioclase, orthoclase, hornblende, and biotite, with SiO₂ content ranging from 59% to 75%. The magmas exhibit medium- to high-K calc-alkaline characteristics, with elevated Rb, Th, and REE concentrations, and initial Sr isotopic ratios of 0.705 to 0.707, indicating a mix of mantle and crustal sources. Geochronological dating suggests emplacement ages between 92 and 109 Ma [2] [1]. [6] classified the Dinh Quan – Deo Ca suites (BH, BN-BD, and BN-PD) as I-type granite related to Paleo-Pacific subduction (110 – 90 Ma).

The Ankoet granitoid complex ($\gamma K_2 ak$) is also located within the Da Lat structure and comprises biotite granite, and adamellite. Its mineralogy features quartz, plagioclase, and K-feldspar, with SiO₂ content between 70% and 76% and a K₂O/Na₂O ratio of approximately 1.4. This complex intrudes and metamorphoses the La Nga formation sediments, granodiorite of the Dinh Quan-Deo Ca complex, and felsic volcanic rocks of the Don Duong formation. It is overlain by Neogene-Quaternary basalt, with Late Cretaceous ages ranging from 85 to 96 Ma [2] [4]. According to [6], the igneous suites from the Ankoet complex (CD, PA, and NS-AB) exhibit A-type granite characteristics, suggesting a link to the transition crust extension phase (83 – 75 Ma) that followed the Paleo-Pacific subduction.

As reported in [6], the Bay Nui-Ba Den diorite suite includes monzogabbro, monzodiorite, diorite, and syenite, with plagioclase, olivine, pyroxene, K-feldspar, amphibole, and biotite as major minerals; Accessory minerals are apatite, titanite, magnetite, and ilmenite. The Bay Nui-Phnom Den granitoid suite comprises granodiorite, quartz monzonite, monzogranite, granite, pegmatite, and aplite; major minerals include plagioclase, K-feldspar, quartz, biotite, and amphibole; accessory minerals are titanite, magnetite, allanite, and apatite. The Pha Aok granitoid suite features two-mica granite with orthoclase, microcline, quartz, and K-feldspar phenocrysts; accessory minerals include fluorite and monazite. The Nui Sam-Angkor Borei granitoid suite includes fine- to medium-grained granites with quartz, K-feldspar phenocrysts, and sericitized plagioclase; accessory minerals are fluorite and ilmenite. Bach Ho granitoid suite (offshore rocks), contain granodiorite and granite with plagioclase, K-feldspar, quartz, and amphibole; accessory minerals are titanite, epidote, apatite, and allanite. The Con Dao gabbro/granite suite (offshore rocks) features fine-grained granite with plagioclase, K-feldspar, quartz, amphibole, pyroxene, and biotite; accessory minerals are magnetite, ilmenite, and apatite.

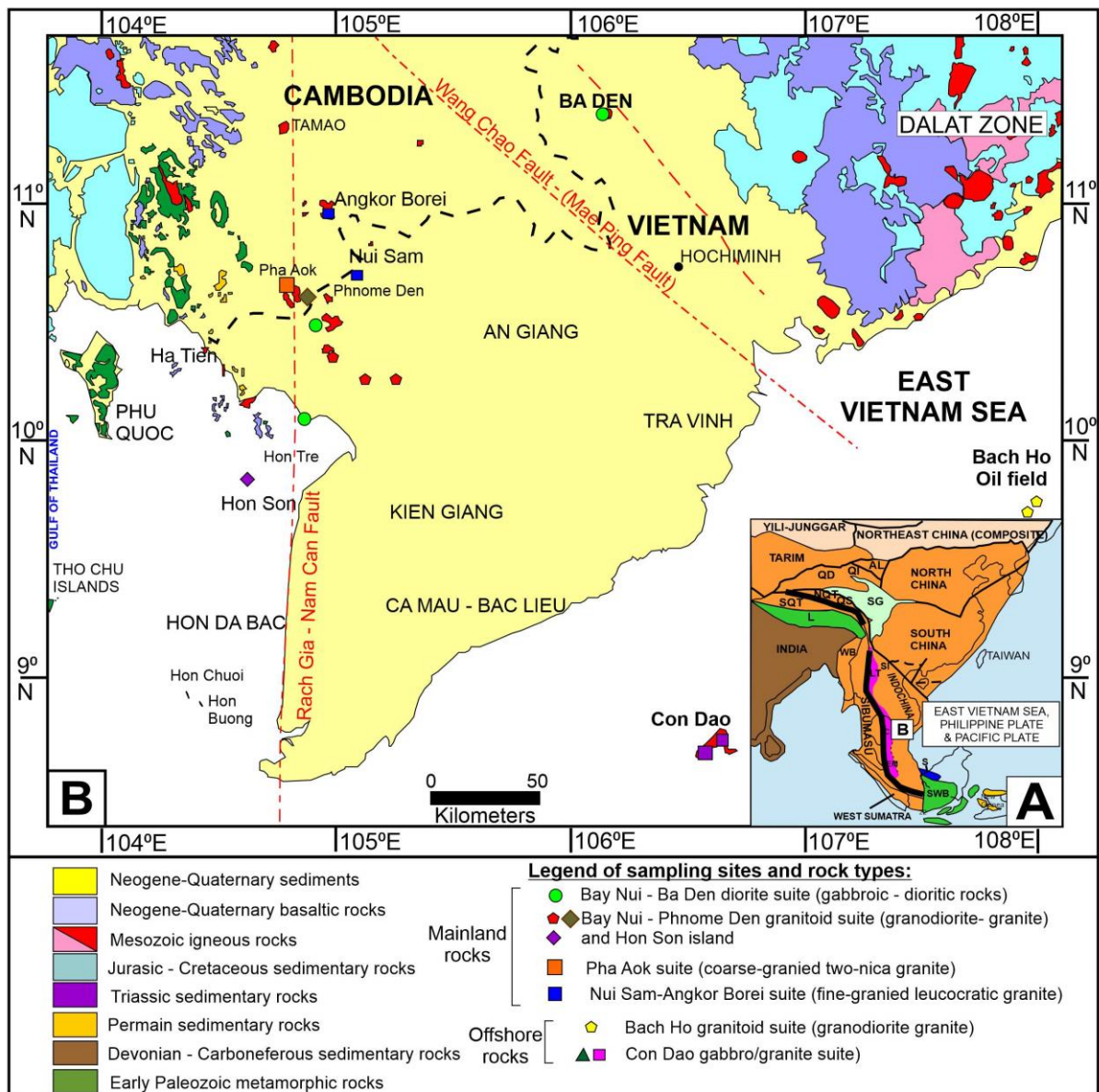


Fig. 1. Simplified geological settings of (A) Southeast Asia and (B) the Dinh Quan-Deo Ca – Ankrøet granitoids in southwest Vietnam and southeast Cambodia (Modified after [6], [25], and [26]).

3. Methodology

3.1. Biotite as an indicator of emplacement parameters

Biotite is a prevalent mineral found in nearly all granitic rocks associated with the Dinh Quan – Deo Ca – Ankoets granites [6]. The characteristics of "primary magmatic biotite" [12] in calc-alkalic granite provide valuable insights into various geological conditions, such as temperature of crystallization [13], pressure condition [14], and redox state (fugacity oxygen, [8] [9]). The structural formulas for biotite have been established based on the equivalents of 22 oxygens and 13 cations, excluding H₂O⁺, as detailed by [27]. As noted by [6], the granites of the Dinh Quan – Deo Ca – Ankoets region are classified within the calc-alkaline suite; thus, as a differ from the work of [6] this research specifically examines the composition of biotite identified as "primary magmatic biotite" from these granitic formations [12] (Fig. 2a).

The crystallization temperature of biotite in granitic environments can be determined utilizing the equation (1) proposed by [13] as follow:

$$T(K) = \frac{838}{1.0337 - \frac{\text{Ti}}{\text{Fe}^{2+}}} \quad (1)$$

Additionally, the Al-in-biotite technique provides a robust means for assessing the emplacement pressure during the crystallization of biotite. This method is recognized as a more dependable geobarometer relative to the Al-in-hornblende approach due to its frequent presence in granitic formations [14]. Pressure calculations can be derived using the following formula:

$$P \text{ (kbar)} = 3.33Al^T - 6.53 (\pm 0.33) \quad (2)$$

Oxygen fugacity (*f*O₂) is essential for understanding magmatic processes, affecting crystallization and melt properties. It determines the redox state during petrogenesis. The calculation of *f*O₂ involves the Fe²⁺-Fe³⁺-Mg²⁺ composition of biotite and specific temperature and pressure conditions. Equation (3) calculates *f*O₂ using coefficients A, B, and C for different oxygen buffers. [9] ternary diagram maps biotite composition, identifying QFM, NNO, and HM buffers based on experimental data. Coefficients for *f*O₂ are selected based on Fe²⁺, Fe³⁺, and Mg²⁺ proportions using methods by [28] and data from [29].

$$\text{Log}fO_2 = -\frac{A}{T} + B + C \frac{(P-1)}{T} \quad (3)$$

3.2. Stimulate the magma chamber using Rhyolite-MELTS program

Rhyolite-MELTS is a valuable thermodynamic modeling tool for assessing the petrological evolution of silicic magma systems [15]. This modified version of MELTS accurately models phase relations in hydrous silicic systems by incorporating additional parameters. Rhyolite-MELTS (version 1.1.0) allows users to simulate phase relations, compositions, and magma chamber parameters, including pressure, temperature, and oxidation state (*f*O₂). It has been applied to study various phenomena, such as quartz-bearing silicic melts and the effects of pressure on saturation surfaces. Users can adjust input parameters to analyze liquid/solid evolution and phase relations. Constraining the petrological conditions for the formation of the Dinh Quan – Deo Ca – Ankoet granitoids is essential for determining optimal modeling parameters. The modeling results are compared with granitic rocks compiled from the studies of [6]. Input data was selected based on the value of Loss on ignition (LOI) < 2.5 wt.%, the range of input P-T condition was adopted from the estimation magmatic condition using the biotite as an indicator in this research, and the hydrated water content (5 wt.%) was chosen regarding of the subduction tectonic setting (Tab. 1).

Tab. 1. Parental composition and conditions used for the Rhyolite MELTS models of the Dinh Quan – Deo Ca – Ankoet granitoids.

Oxides (wt.%)	Dinh Quan – Deo Ca – Ankoet granitoids				
	BN12-1 [6]	BN14 [6]	BH150 [6]	CD155 [6]	PA118 [6]
SiO ₂ (wt.%)	66.36	65.6	64.69	50.36	72.63
TiO ₂	0.34	0.36	0.61	0.87	0.21
Al ₂ O ₃	15.53	16.17	16.45	16.98	13.86

FeO _t	3.36	3.35	3.58	7.89	2.23
MnO	0.09	0.09	0.066	0.142	0.01
MgO	1.56	1.45	1.38	7.08	0.71
CaO	3.94	4.09	4.48	9.9	1.08
Na ₂ O	3.06	3.39	3.88	2.69	3.47
K ₂ O	4.34	4.2	2.12	0.59	5.36
P ₂ O ₅	0.17	0.17	0.207	0.078	0.01
H ₂ O _{initial}	5 (wt.%)	5 (wt.%)	5 (wt.%)	5 (wt.%)	5 (wt.%)
<i>f</i> O ₂	FMQ -3	FMQ -1	FMQ +1	FMQ -3	FMQ-1
Temperature (°C)	1300	1300	1300	1300	1300
Pressure (GPa)	0.3	0.3	0.3	0.4	0.35

QFM = quartz-fayalite-magnetite buffer.

All major elements data for models normalized to 100% including water.

4. Results and Discussion

4.1 Estimation of magmatic condition

The results of crystallization temperature, pressure, and redox state estimate from 16 biotite grains of Dinh Quan – Deo Ca – Ankoet granitic rocks are listed in Tab. 2.

Tab. 2. Estimation of crystallization temperature, pressure, and redox state of Dinh Quan – Deo Ca – Ankoets granitic rocks using biotite as an indicator. (The chemistry of the biotite was reported in [6]).

Complex	Sample name	T(°C)	P (GPa)	Log <i>f</i> O ₂ (using QFM buffer)	ΔFMQ
Bay Nui-Ba Den suite	12.2_20.5	749	0.097	-16.43	-0.98
	12.2_21.5	761	0.117	-16.12	-6.30
Bay Nui-Phnom Den suite	14_12.5	759	0.085	-16.18	-6.30
	38.1_14.4	707	0.031	-17.57	-0.96
	38.1_16.2	712	0.085	-17.43	-1.01
	106_1_3	628	0.096	-20.03	-1.11
	106_2_8-large	636	0.068	-19.77	-0.97
Pha Aok suite	119_11.2	615	0.35	-20.48	-1.39
	119_7.1	626	0.311	-20.11	-1.34
	119_8.1	612	0.381	-20.57	-1.43
	119_8.4	605	0.408	-20.81	-1.47
Nui Sam-Angkor Borei suite	43.1_33.3trang	603	0.316	-20.88	-1.37
	43.1_33.4trang	608	0.292	-20.71	-1.34
Bach Ho suite	157_2.1	642	0.272	-19.58	-1.27
	157_5.2	642	0.262	-19.55	-1.26

Note: 1 GPa = 10 kbars (1 gigapascals = 10 kilobars).

The magmatic biotite thermometry for BN-BD diorites, ranging from ~749°C to ~761°C, aligns well with the zircon saturation temperatures ($T_{Zr} = 750^\circ\text{C}$ to 790°C) calculation using method reported by [30] based on whole-rock data from [6]. These temperature estimates from biotite are considered reliable since they tend to be lower than the crystallization temperature of zircon [31]. Pressure estimates for BN-BD dioritic rocks, ranging from ~0.097 to ~0.197 GPa, suggest emplacement depths between ~3.7 km and ~7.5 km. Variability in these pressure estimates could be attributed to biotite redistribution during emplacement. The oxidation state of biotite, determined using Fe²⁺-Fe³⁺-Mg components and recalculated by [28], indicates that biotite from BN-BD dioritic rocks falls within the Quartz-Fayalite-Magnetite (QFM) buffer (Figure 2b). The log *f*O₂ values range from -16.43 to -16.12, corresponding to ΔFMQ = -6.3 to -1,

reflecting reduced conditions. However, the chemical composition of BN-BD biotite is predominantly reported from of dioritic rocks [6] which is not identical to the calc-alkaline granites [12]; therefore, these values should be used only as reference. The biotite thermometry estimates for BN-PD granite (~749°C to ~761°C) fall within the T_{Zr} ranging from 735°C to 837°C. Pressure estimates for BN-PD granites range from ~0.031 to ~0.096 GPa, indicating emplacement depths between ~1.2 km and ~3.6 km. The oxidation state estimations, with recalculated values, show reduced conditions with $\Delta FMQ = -6.3$ to -1 . For BH granites, biotite thermometry is estimated at 642°C, which is lower than the T_{Zr} which ranging from 752°C to 777°C). Pressure estimates range from ~0.26 to ~0.27 GPa, suggesting emplacement depths between ~9.8 km and ~10.2 km.

PA granites have biotite thermometry estimates ranging from 605°C to 626°C, lower than the T_{Zr} which ranging from 746°C to 810°C. Pressure estimates range from ~0.31 to ~0.41 GPa, indicating emplacement depths between ~11.7 km and ~15.5 km, with reduced conditions ($\Delta FMQ = -1.3$ to -1.5). NS-AB granites exhibit biotite thermometry estimates from 603°C to 608°C, lower than the T_{Zr} which ranging from 704°C to 706°C. Pressure estimates range from ~0.29 to ~0.32 GPa, suggesting emplacement depths between ~11.0 km and ~12.1 km. Finally, [6] reports only the biotite from the CD gabbro, which precludes the application of the Al-in-biotite geobarometer for estimating the magmatic conditions of the CD granite.

The pressure estimation using biotite as an indicator are at lower values comparing to the Al-in-hornblende method which has been reported in [6] which is reliable as biotite crystallized after amphibole as described in Bowen reaction series [32].

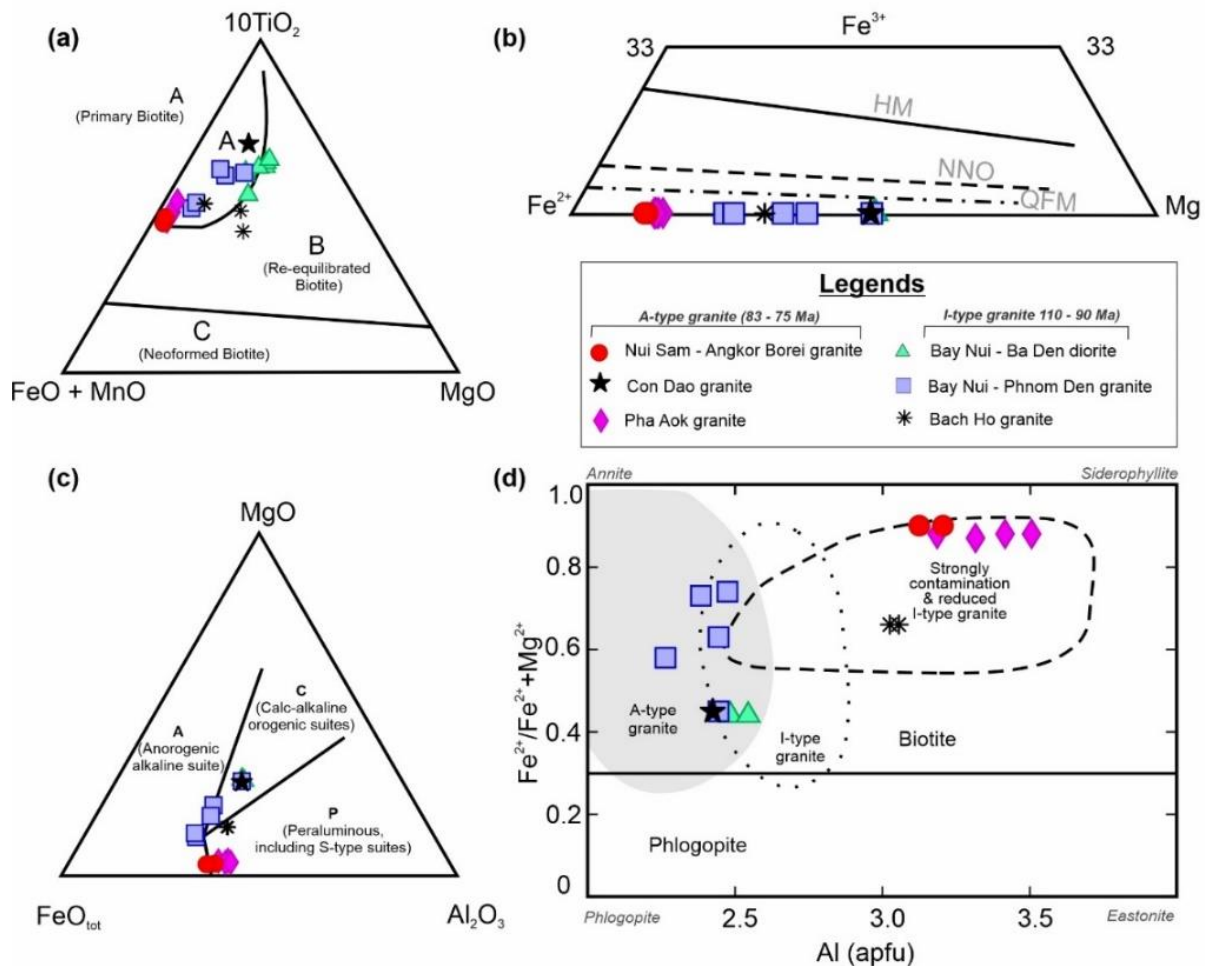


Fig. 2. (a) Classification of primary magmatic biotite as described by [33]. (b) Biotite redox conditions plotted following [9] [8]. (c) Diagram of tectonomagmatic discrimination for biotite according to [7]. (d) Diagram of biotite discrimination using $Fe^{2+}/(Fe^{2+}+Mg^{2+})$ and total aluminum (Al_{tot} , in atomic formula units per formula unit, apfu) based on [8].

4.2. Fraction crystallization models

The compositional patterns of major elements in granitic, granodioritic, and dioritic rocks, as detailed by [6], indicate that the BN-BD, BN-PD, BH, NS-AB, PA, and CD might be members of related intrusive compositions. Additionally, trace element analyses suggest the involvement of fractional crystallization processes involving clinopyroxene, amphibole, feldspar, and garnet [6]. To investigate the genetic links among the dioritic, granodioritic, and granitic rocks within the Dinh Quan – Deo Ca – Ankoet granitic suites, melting-fractionation simulations were performed using Rhyolite-MELTS version x1.1.0 [15], with the granodioritic or most primitive composition of each suite serving as the initial magma (Tab. 1).

Simulations were conducted under conditions reflective of the middle to upper crust (0.3 to 0.4 GPa), utilizing biotite chemistry to estimate pressure, temperature, and redox states. The models were hydrous, with water content set as 5 wt.%. Various parameter combinations were tested to assess potential derivation pathways from the dioritic, granodioritic, and granitic rocks. The results of the six most effective models are illustrated in Figures 3, 4, and 5. Generally, the model curves for residual liquid compositions align with the compositional range of the Dinh Quan – Deo Ca – Ankoet granitic suites, with the exception of model CDFC4, which utilized the initial composition of the CD gabbro. Each model's liquid evolution curve intersects the central data range for the respective suites (Fig. 3). The details of each model are presented in the Supplementary data, from Table S1 to Table S8.

For I-type granites, the model initiated with the BN12-1 composition first yields a composition akin to BN-PD granite at 1005°C, with a liquidus temperature of 1006°C, resulting in approximately 99.7% melt remaining at the first solid composition comparable to Dinh Quan – Deo Ca – Ankoet granitic rocks (Fig. 4). These findings support that BN-PD granite can be generated through the fractionation of BN-PD granodiorite. Similarly, the model beginning with BN-14 produces a composition resembling BN-PD granite at 980°C, with a liquidus temperature of 981°C, retaining about 99.6% melt at the initial solid composition equivalent to BN-PD granite (Fig. 4). This suggests that the primary composition for BN-PD may closely resemble sample BN-14. The modeling indicates that BN-PD granite can indeed originate from the fractionation of BN-PD granodiorite (sample BN-14). For the model BHFC2 (which use the sample BH150 as parental magma), the fraction crystallization process shows that the liquidus composition trend intersects both the BH granites and the broader granitic compositions of the Dinh Quan – Deo Ca – Ankoet suites, with the first solid phase forming at 957°C (Fig. 4) and a melt composition of approximately 99.4% (Tab. S4). All models were computed at a pressure of 0.3 GPa, suggesting an upper crustal emplacement depth of around 11.3 km.

In the case of A-type granite, isobaric fractional crystallization of PA granodiorite (sample PA118) was also conducted, with the liquidus composition trend passing through the PA granites and much of the granitic compositions of the Dinh Quan – Deo Ca – Ankoet suites, where the first solid phase forms at 938°C (Fig. 5) and retains about 99.4% melt. In contrast, the isobaric fractional crystallization of CD gabbro (sample CD155) shows a liquidus composition curve that traverses the ranges of BH and BN-PD granites before reaching the granitic composition of the CD suite, with the first solid phase appearing at 1175°C (Fig. 5) and a melt composition of approximately 99.7%. The results from model CDFC4 suggest that the Dinh Quan – Deo Ca – Ankoet granitic suites might have formed through polybaric fractional crystallization, beginning with a gabbroic/basaltic composition similar to the CD gabbro at a middle crust depth of approximately 15 km, followed by the fractionation of the granodioritic composition.

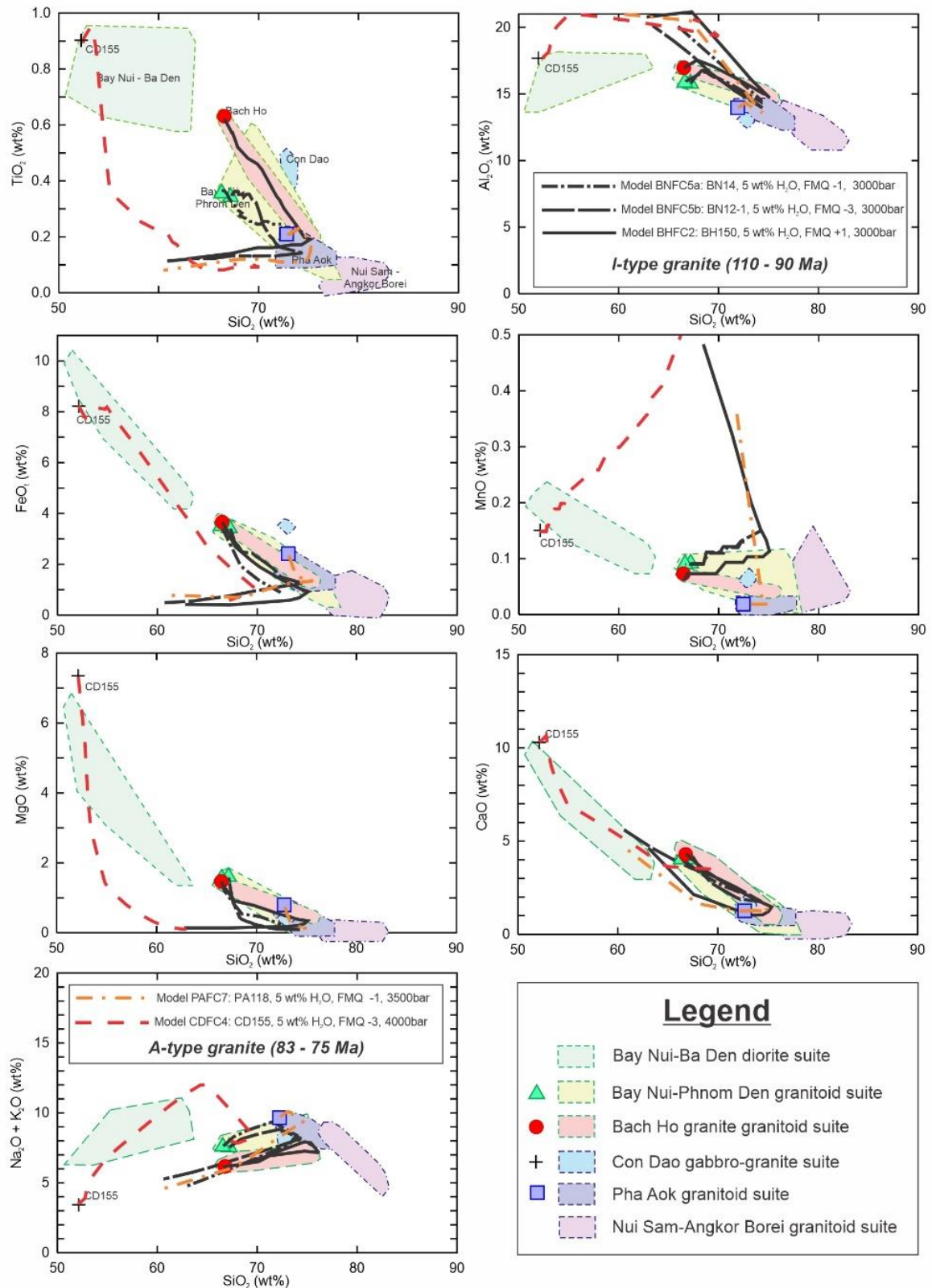
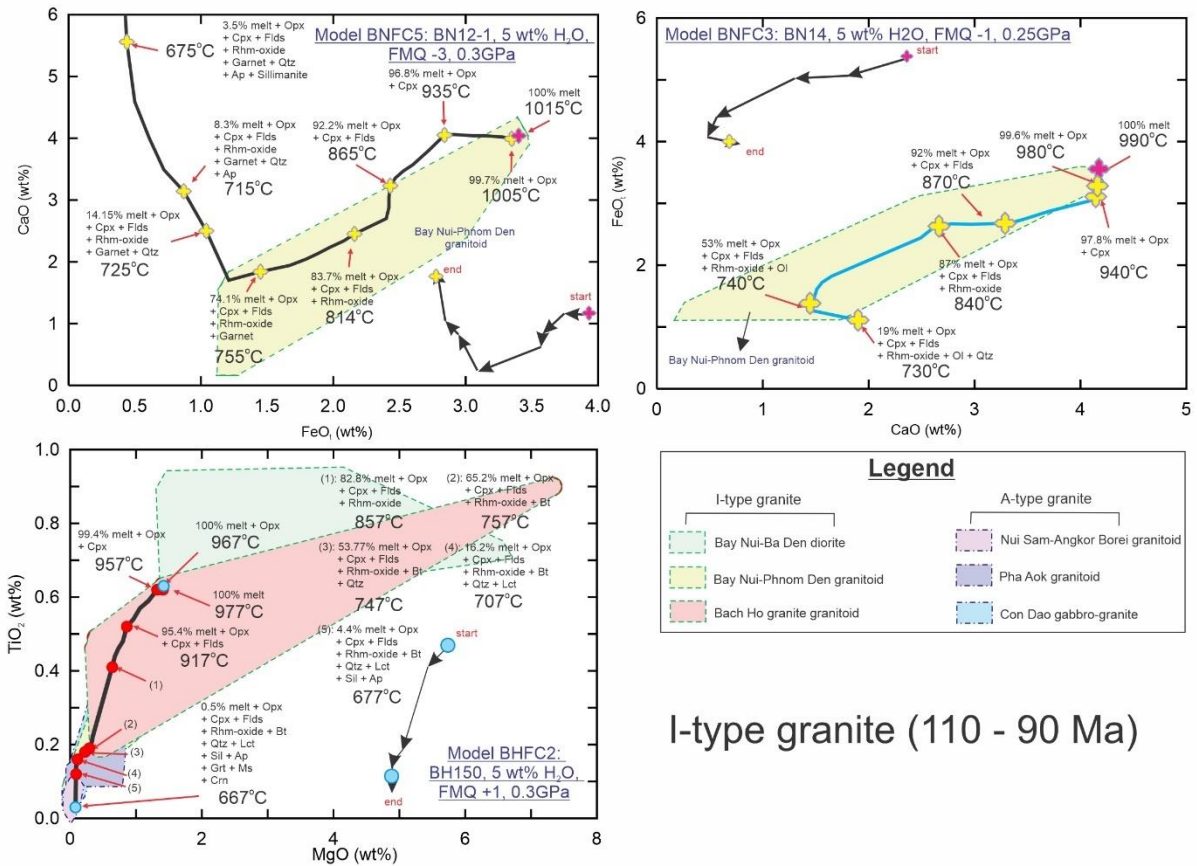


Fig. 3. Major element liquid evolution of fractional crystallization modeling using the of the Dinh Quan - Deo Ca - Ankrøet granitic rocks as parental magma compositions.



I-type granite (110 - 90 Ma)

Fig. 4. Crystallization phases of each I-type granite pluton generated for Rhyolite MELTS models. [15]

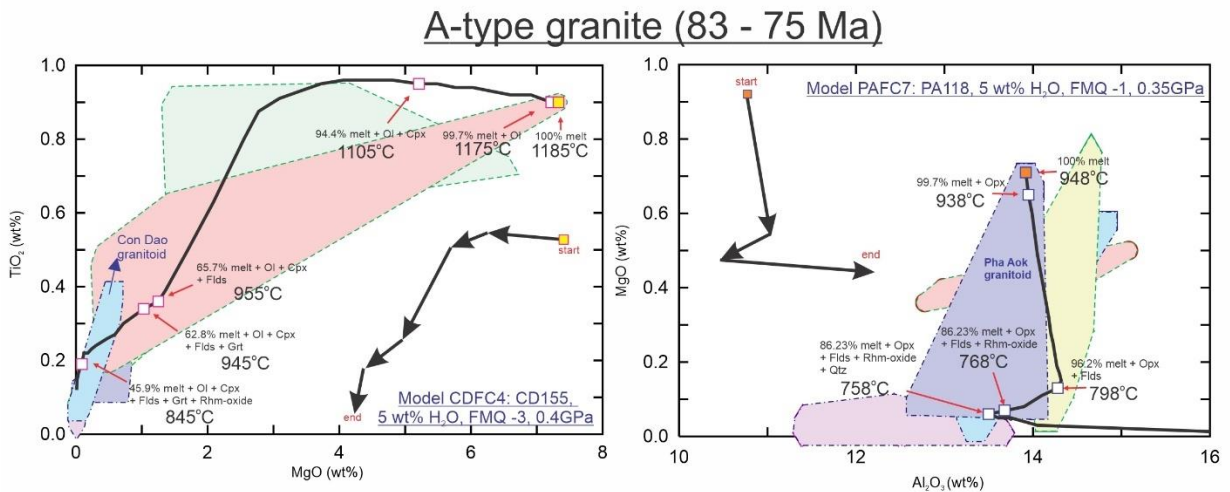


Fig. 5. Crystallization phases of each A-type granite/ SCR I-type granites pluton generated for Rhyolite MELTS models. [15]

4.3. Implications for the tectonic settings and formation of the rocks

The composition of biotite serves as a valuable tool for inferring the tectonic settings of host rocks. This study builds upon the tectonomagmatic classifications established by [7] and [8], particularly focusing on the characteristics of "primary magmatic biotite" as refined by [12]. This study's findings indicate that the older granitic suites, specifically the I-type BN-BD and BN-PD granites, predominantly exhibit calc-alkaline orogenic characteristics (Fig. 2c). Notably, two samples from the BN-PD suite align with an anorogenic alkaline classification, while the BH granites are classified as peraluminous. The distinction between I-type granites and their proximity to the A-type granite field is evident, with the BH granites

demonstrating features consistent with strongly contaminated and reduced (SCR) I-type granites (Fig. 2d). The geochemical analysis of biotite in these 110-90 Ma I-type granites correlates closely with the whole-rock geochemical classifications reported by [6], reinforcing the reliability of biotite as a tectonic indicator. In contrast, the younger 83-75 Ma A-type granites, particularly the CD suite, also fall within the calc-alkaline orogenic category, yet are distinctly classified as A-type. The PA and NS-AB granites are identified as peraluminous, paralleling the classifications derived from whole-rock geochemistry by [6]. In contrast to the A₂-type granitic classification put forth by [6], the biotite discrimination method described by [8] classifies the PA and NS-AB granites as SCR I-type. [34] [35] posited that A₂-type granites are post-orogenic and result from crustal melting and mixing with mantle sources, which resonates with the characteristics of SCR I-type granites.

The geochronological data presented by [6] delineates the emplacement ages of the various granite suites: (1) I-type granites associated with Paleo-Pacific subduction—BH at 110 Ma, BN-BD from 107-96 Ma, and BN-PD around 94-91 Ma; (2) A-type/ SCR I-type granites related to transitional crust extension phase which is prior to the sea-opening in Cenozoic —CD at 83 Ma, PA at 78 Ma, and NS-AB at 75 Ma. This chronological framework, when integrated with the biotite geochemical discrimination techniques, reveals insights into the evolution and transition of the parental magma compositions that led to the formation of the Dinh Quan – Deo Ca – Ankroet granitic rocks. The subduction of the Paleo-Pacific plate beneath the Eurasian plate likely initiated the melting of oceanic crust materials, which subsequently ascended to mid- to upper-crustal depths (approximately 3.7 km to 11.3 km). This process, coupled with interactions with the lower crust, produced heterogeneous parental magmas characterized as strongly contaminated and reduced (SCR, BH granite). As mixing progressed, a more homogeneous source emerged, leading to the fractionation that produced the BN-BD and BN-PD granitic rocks. The extensional tectonic regime provided additional thermal energy, facilitating the injection of basaltic magma from the mantle, which resulted in partial melting of the lower crust, giving rise to the CD granite at mid-crustal depths (~15 km). Continued thermal input further enhanced partial melting, resulting in the formation of SCR I-type granites represented by the NS-AB and PA granites at depths of approximately 13 – 15 km (Fig. 6).

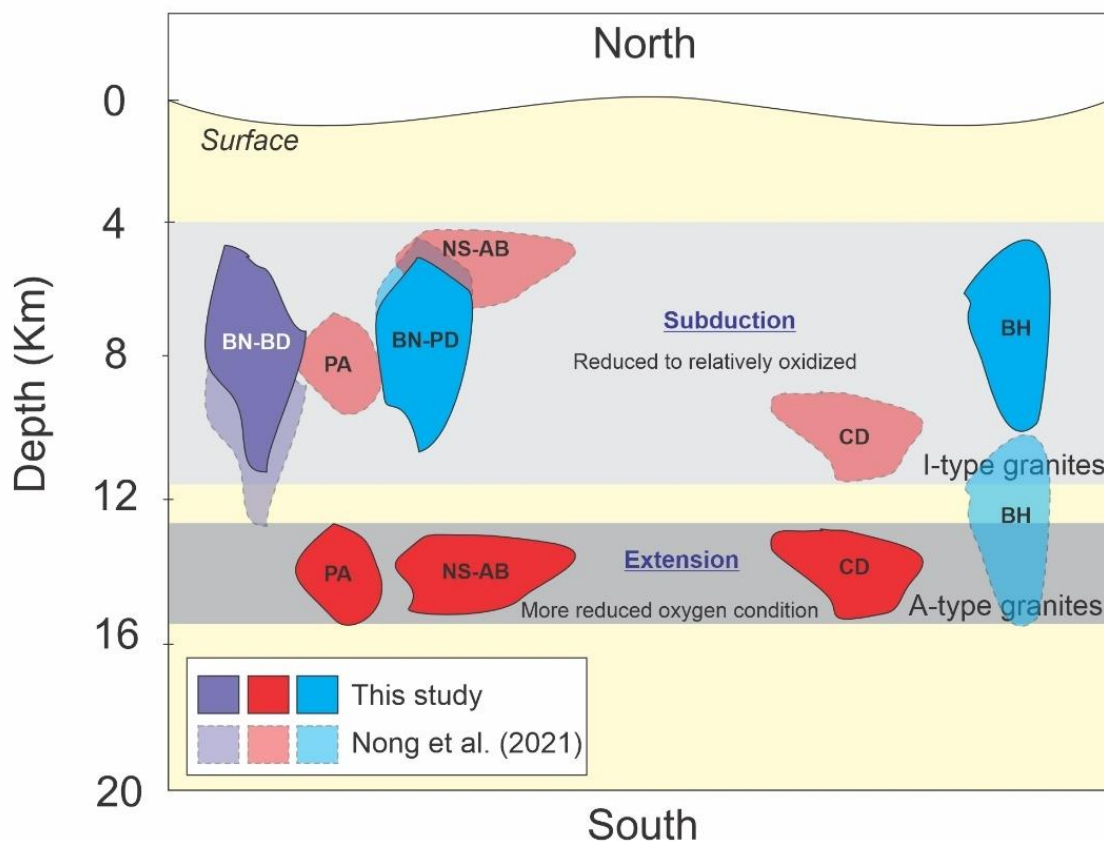


Fig. 6. A conceptual model illustrating the tectono-magmatic processes involved in the crustal evolution of the Dinh Quan – Deo Ca – Ankroet granitoids, SW Vietnam and SE Cambodia.

5. Conclusion

This study employs the Al-in-biotite geobarometer alongside Rhyolite MELTs modeling to elucidate the magmatic conditions of the Dinh Quan – Deo Ca – Ankroet I-type and A-type/ SCR I-type granites found within the SW Vietnam-SE Cambodia region. The findings provide significant insights into the regional tectonic framework and the evolution of the parental magmas. The key findings are summarized as follows:

- The Al-in-biotite method indicates that the magmatic conditions for I-type granitic rocks range from pressures of 0.03 to 0.27 GPa and temperatures between 628 and 759°C, under reduced condition ($\Delta\text{FMQ} = -6.3$ to -1). In contrast, A-type/ SCR I-type granites exhibit pressures of 0.31 to 0.41 GPa, temperatures ranging from 603 to 626°C, and under reduced condition ($\Delta\text{FMQ} = -1.5$ to -1.3).
- The Al-in-biotite method indicates that the NS-AB and PA granites, previously classified as A-type, exhibit characteristics of peraluminous, highly contaminated, and reduced I-type granites. (SCR I-type granites). These findings underscore the necessity for a comprehensive investigation into their petrogenesis and tectonic significance.
- Rhyolite MELTs modeling suggests that I-type granitic rocks crystallized at a pressure of approximately 0.3 GPa and temperatures between 1005 and 730°C, under relatively reduced oxygen conditions ($\Delta\text{FMQ} -1$), except for the BH granitoid, which shows a more oxidized condition ($\Delta\text{FMQ} +1$). A-type/ SCR I-type granites formed under pressures of 0.35 to 0.4 GPa and temperatures from 1175 to 758°C, characterized by stronger reduced oxygen conditions ($\Delta\text{FMQ} -3$ to $\Delta\text{FMQ} -1$).
- The magmatic condition estimation from Al-in-biotite geobarometer method can be used to control the input values for Rhyolite MELTs models to generate the fraction crystallization process of the Dinh Quan – Deo Ca – Ankroet I-type and A-type/ SCR I-type granites found within the SW Vietnam-SE Cambodia region.
- The I-type granitic rocks associated with Paleo-Pacific subduction (110 – 90 Ma) were emplaced at depths ranging from 3.7 to 11.3 km, under relatively reduced oxygen conditions. In contrast, the A-type granites/ SCR I-type granites resulting from transitional crust extension phase (83 – 75 Ma) formed at greater depths of 11 to 15.5 km, exhibiting distinctively stronger reduced oxygen conditions.

Acknowledgements

This research is funded by the University of Science, VNUHCM under grant number T2023 – 142. Author thank the anonymous reviewers for improving the submission. Ms. Nguyen Kim Truc Linh and Mr. Nguyen Van Long Thanh are appreciated for their assistance in illustrating the models.

Literature - References

1. Nguyen X.B., Vu N.H, Trinh, V.L., "Age correction of some Mesozoic stratigraphic units in South Vietnam. DC, Resources and Environment of South Vietnam," Southern Geodetic Federation, Ho Chi Minh City, pp. 16-19, 2000.
2. Nguyen T.B.T, Siebel W., Satir M., Bui M.T., "Internal structure of zircons and U-Pb geochronological evidence for the existence of a Pre-Cambrian basement in the Da Lat Zone, Southern Viet Nam," *Journal of Geology*, pp. B/19-20: 69-78., 2002.
3. Nguyen, T.B.T., Satir, M., Siebel, W., Vennemann, T., Van Long, T., "Geochemical and isotopic constraints on the petrogenesis of granitoids from the Dalat zone, southern Vietnam," *Journal of Asian Earth Sciences*, pp. 23, 467–482, 2004.
4. P. L. Anh, "Petrogenesis of the high aluminum granite association Ca Na," *Journal of Earth Sciences*, pp. 23(4), 311-318, 2001.
5. Tri, T.V., Khuc, V., *Geology and Natural Resources of Vietnam*, Hanoi: Natural Science and Technology Publishing House, 2009.
6. Nong, T.Q.A, Christoph A. Hauzenberger, C.A, Gallhofer. D., Sang Q. Dinh., "Geochemistry and zircon U-Pb geochronology of Late Mesozoic igneous rocks from SW Vietnam– SE Cambodia: Implications for episodic magmatism in the context of the Paleo Pacific subduction," *Lithos*, p. 390–391 (2021) 106101, 2021.
7. M. Abdel-Rahman, "Nature of biotites from alkaline, calc-alkaline, and," *Journal of Petrology*, p. 525–541, 1994.
8. Shabani, A. A. T., Lalonde, A. E., Whalen, J. B., "Composition of biotite from granitic rocks of the Canadian Appalachian orogen: a potential tectonomagmatic indicator?," *The Canadian Mineralogist*, pp. 41, 1381–1396, 2003.
9. Wones, D., Eugster, H., "Stability of biotite: experiment, theory, and application.," *American Mineralogist*, pp. 50, 1228–1272, 1965.

10. D. J. M. Burkhard, "Biotite crystallization temperatures and redox states in granitic rocks as an indicator for tectonic setting," *Geology Mijnbouw*, vol. 71, p. 337–349, 1993.
11. D. J. M. Burkhard, "Temperature and redox path of biotite-bearing intrusives: a method of estimation applied to S- and I-type granites from Australia," *Earth Planetary Science Letters*, vol. 104, pp. 89–98, 1991.
12. Nachit, H., Ibhi, A., Abia, E. H., Ohoud, M. B., "Discrimination between primary magmatic biotites, reequilibrated biotites and neoformed biotites," *Comptes Rendus Geoscience*, pp. 337, 1415–1420, 2005.
13. Luhr, J. F., Carmichael, I. S. E., Varekamp, J. C., "The 1982 eruptions of El Chichon volcano, Chiapas, Mexico-Mineralogy petrology of the anhydrite bearing pumices," *Journal of Volcanology and Geothermal Research*, pp. 23, 69–108, 1984.
14. Uchida, E., Endo, S., Makino, M., "Relationship between solidification depth of granitic rocks and formation of hydrothermal ore deposits," *Resource Geology*, pp. 57, 47–56, 2007.
15. Gualda, G.A.R., Ghiorsso, M.S., Lemons, R. V., Carley, T.L., "Rhyolite-MELTS: A modified calibration of MELTS optimized for silica-rich, fluid-bearing magmatic systems," *Journal of Petrology*, vol. 53, p. 875–890, 2012.
16. Nguyen, T.B.T., Satir, M., Siebel, W., Chen, F., "Granitoids in the Dalat zone, southern Vietnam: age constraints on magmatism and regional geological implications," *International Journal of Earth Sciences*, pp. 93, 329–340., 2004.
17. Shellnutt, J.G., Lan, C.Y., Van Long, T., Usuki, T., Yang, H.J., Mertzman, S.A., Iizuka, Y., Chung, S.L., Wang, K.L., Hsu, W.Y., "Formation of cretaceous Cordilleran and postorogenic granites and their microgranular enclaves from the Dalat zone, southern Vietnam: Tectonic implications for the evolution of Southeast Asia," *Lithos*, pp. 182, 229–241, 2013.
18. M. W. Schmidt, "Amphibole composition in tonalite as a function of pressure: an experimental calibration of the Al-in-hornblende barometer," *Contributions to Mineralogy and Petrology*, pp. 110, 304–310, 1992.
19. X. Yang, "Estimation of crystallization pressure of granite intrusions," *Lithos*, pp. 286, 324–329, 2017.
20. R. Hall, "Late Jurassic-Cenozoic reconstructions of the Indonesian region and the Indian Ocean," *Tectonophysics*, pp. 570–571, 1–41, 2012.
21. Metcalfe, "Tectonic evolution of Sundaland," *Bulletin Of The Geological Society Of Malaysia*, pp. 63, 27–60, 2017.
22. Fyhn, M.B.W., Green, P.F., Bergman, S.C., Van Itterbeeck, J., Tri, T.V., Dien, P.T., Abatzis, I., Thomsen, T.B., Chea, S., Pedersen, S.A.S., Mai, L.C., Tuan, H.A., Nielsen, L.H., "Cenozoic deformation and exhumation of the Kampot Fold Belt and implications for South Indochina tectonics," *Journal of Geophysical Research Solid Earth*, vol. 121, p. 5278–5307, 2016.
23. C. Morley, "Late Cretaceous-early Palaeogene tectonic development of SE Asia," *Earth-Science Reviews*, pp. 115, 37–75, 2012.
24. Hoang, N., Flower, M.F., Xuân, P.T., Quy, H.V., Son, T.T., "Collision-induced basalt eruptions at Pleiku and Buôn Mê Thuột, south-Central Viet Nam," *Journal of Geodynamics*, pp. 69, 65–83, 2013.
25. Metcalfe, "Tectonic framework and Phanerozoic evolution of Sundaland," *Gondwana Research*, vol. 19, no. 1, pp. 3–21, 2011.
26. Metcalfe, "Gondwana dispersion and Asian accretion: Tectonic and palaeogeographic evolution of eastern Tethys," *Journal of Asian Earth Sciences*, vol. 66, p. 1–33, 2013.
27. Tindle, A. G., Webb, P. C., "Estimation of lithium contents in trioctahedral micas using microprobe data: applications to micas from granitic rocks," *European Journal of Mineralogy*, pp. 2, 595–610, 1990.
28. P. I. Nenova, "'Fe23": a computer program for calculating the number of Fe²⁺ and Fe³⁺ ions in minerals," *Computers & Geosciences*, pp. 23, 215–219, 1997.
29. Eugster, H. P., Wones, D. R., "Stability reactions of the ferruginous biotite, annite," *Journal of Petrology*, pp. 3, 82–125, 1962.
30. Boehnke, P., Watson, E.B., Trail, D., Harrison, T.M., Schmitt, A.K., "Zircon saturation revisited," *Chemical Geology*, vol. 351, p. 324–334, 2013.
31. Harrison, T. M., Watson, E. B., Aikman, A. B., "Temperature spectra of zircon crystallization in plutonic rocks," *Geology*, pp. 35, 635–638, 2007.
32. N. L. Bowen, "The Reaction Principle in Petrogenesis," *Journal of Geology*, vol. 30 (3), p. 177–198, 1922.

33. Nachit, H., Razafimahefa, N., Stussi, J. M., Carron, J. P., "Composition chimiques des biotite et typologie magmatique des granitoïdes," C.R. Acadomic Sciences Paris, pp. Series 2, 301, 813-818, 1985.
34. G. Eby, "The A-type granitoidThe A-type granitoids: A review of their occurrence and chemical characteristics and speculations on their petrogenesis," *Lithos*, vol. 26, no. 1-2, pp. 115-134, 1990.
35. G. Eby, "Chemical subdivision of the A-type granitoids: petrogenetic and tectonic implications," *Geology*, pp. 20, 641–644., 1992.

SUPPLEMENTARY DATA

FRACTION CRYSTALLIZATION MODELS

S1. Legends

S2. Model PAFC7: PA118, 5 wt% H₂O, FMQ -1, 0.35 GPa

S3. Model CDFC4: CD155, 5 wt% H₂O, FMQ -3, 0.4 GPa

S4. Model BHFC2: BH150, 5 wt% H₂O, FMQ +1, 0.3 GPa

S5. Model BNFC5a: BN14, 5 wt% H₂O, FMQ -1, 0.3 GPa

S6. Model BNFC5b: BN12-1, 5 wt% H₂O, FMQ -3, 0.3 GPa

S7. Model BNFC3: BN14, 5 wt% H₂O, FMQ -1, 0.25 GPa

S8. Crystallization Phases

Notes: The results presented within this appendix are the output data generated by Rhyolite-MELTS for hydrous (H₂O = 5 wt%) fractional crystallization of the composition listed in Table 1.

S1. Legends

T = Temperature (°C)

Ol = Olivine

Opx = Orthopyroxene

Cpx = Clinopyroxene

Flds = Feldspars

Qtz = Quartz

Rhm-oxide = (hematite, ilmenite, gieselerite, pyrophanite)

Spi = Spinel

Bt = Biotite

Ap = Apatite

S2. Model PAFC7: PA118, 5 wt% H₂O, FMQ -1, 0.35 GPa

T (°C)	Model PAFC7 – Normalized liquid composition (wt%)										
	SiO ₂	TiO ₂	Al ₂ O ₃	FeO _t	MnO	MgO	CaO	Na ₂ O	K ₂ O	P ₂ O ₅	Total
937.89	73.01	0.21	13.95	2.18	0.01	0.65	1.08	3.50	5.40	0.01	100.00
927.89	73.06	0.21	13.99	2.12	0.01	0.60	1.09	3.50	5.41	0.01	100.00
917.89	73.11	0.21	14.02	2.06	0.01	0.55	1.09	3.51	5.42	0.01	100.00
907.89	73.16	0.21	14.05	2.00	0.01	0.49	1.09	3.52	5.44	0.01	100.00
897.89	73.22	0.21	14.09	1.94	0.01	0.44	1.09	3.53	5.46	0.01	100.00
887.89	73.27	0.21	14.12	1.87	0.01	0.40	1.09	3.54	5.47	0.01	100.00
877.89	73.33	0.21	14.15	1.81	0.01	0.36	1.09	3.54	5.48	0.01	100.00
867.89	73.39	0.21	14.18	1.75	0.01	0.32	1.09	3.55	5.49	0.01	100.00
857.89	73.43	0.21	14.20	1.69	0.01	0.28	1.10	3.57	5.50	0.01	100.00
847.89	73.46	0.22	14.23	1.62	0.01	0.25	1.10	3.57	5.52	0.01	100.00
837.89	73.51	0.22	14.25	1.56	0.01	0.22	1.10	3.58	5.53	0.01	100.00
827.89	73.56	0.22	14.27	1.50	0.01	0.19	1.10	3.59	5.54	0.01	100.00
817.89	73.62	0.22	14.30	1.44	0.01	0.17	1.10	3.59	5.54	0.01	100.00
807.89	73.65	0.22	14.32	1.39	0.01	0.15	1.10	3.60	5.55	0.01	100.00
797.89	73.77	0.22	14.28	1.32	0.01	0.13	1.08	3.57	5.60	0.01	100.00
787.89	74.12	0.23	14.10	1.29	0.01	0.11	1.05	3.50	5.58	0.01	100.00
777.89	74.54	0.23	13.90	1.27	0.01	0.08	1.05	3.44	5.47	0.01	100.00
767.89	75.03	0.19	13.68	1.21	0.01	0.07	1.04	3.39	5.37	0.01	100.00
757.89	75.42	0.18	13.50	1.17	0.01	0.06	1.04	3.34	5.26	0.01	100.00
747.89	75.33	0.15	13.61	1.17	0.01	0.05	1.08	3.41	5.18	0.01	100.00
737.89	75.19	0.13	13.75	1.18	0.01	0.05	1.12	3.48	5.08	0.01	100.00
727.89	74.82	0.11	14.05	1.33	0.02	0.03	1.09	3.61	4.91	0.02	100.00
717.89	72.31	0.11	17.06	1.03	0.35	0.00	1.07	2.75	4.94	0.38	100.00
707.89	70.72	0.12	18.90	0.81	0.53	0.00	1.22	2.12	5.00	0.58	100.00
697.89	69.38	0.12	20.39	0.65	0.67	0.00	1.35	1.72	4.98	0.74	100.00
687.89	68.18	0.12	21.72	0.52	0.79	0.00	1.47	1.42	4.92	0.87	100.00
677.89	60.64	0.08	22.36	0.61	3.08	0.00	4.59	1.64	3.57	3.44	100.00
667.89	24.89	0.02	14.77	0.64	16.72	0.00	22.55	0.97	0.74	18.70	100.00
657.89	22.53	0.02	13.32	0.52	17.96	0.00	24.19	0.78	0.57	20.10	100.00

S3. Model CDFC4: CD155, 5 wt% H₂O, FMQ -3, 0.4 GPa

T (°C)	Model CDFC4 – Normalized liquid composition (wt%)										
	SiO ₂	TiO ₂	Al ₂ O ₃	FeO _t	MnO	MgO	CaO	Na ₂ O	K ₂ O	P ₂ O ₅	Total
1175.2	52.18	0.90	17.64	8.15	0.15	7.22	10.28	2.79	0.61	0.08	100.00
1165.2	52.29	0.92	17.78	8.08	0.15	6.91	10.36	2.82	0.62	0.08	100.00
1155.2	52.39	0.92	17.93	8.02	0.15	6.60	10.45	2.84	0.62	0.08	100.00
1145.2	52.49	0.93	18.07	7.95	0.15	6.31	10.53	2.87	0.63	0.08	100.00
1135.2	52.59	0.94	18.21	7.88	0.15	6.03	10.60	2.89	0.63	0.08	100.00
1125.2	52.69	0.94	18.35	7.81	0.15	5.76	10.68	2.91	0.63	0.08	100.00
1115.2	52.79	0.95	18.48	7.73	0.15	5.49	10.76	2.93	0.64	0.08	100.00
1105.2	52.87	0.95	18.67	7.68	0.15	5.21	10.76	2.97	0.65	0.08	100.00
1095.2	52.92	0.96	19.19	7.74	0.16	4.81	10.38	3.07	0.68	0.08	100.00
1085.2	52.99	0.96	19.68	7.82	0.16	4.43	10.00	3.17	0.70	0.10	100.00
1075.2	53.06	0.96	20.16	7.88	0.16	4.06	9.64	3.27	0.72	0.10	100.00
1065.2	53.15	0.95	20.62	7.92	0.17	3.72	9.27	3.36	0.74	0.10	100.00
1055.2	53.26	0.93	21.06	7.96	0.17	3.40	8.92	3.45	0.77	0.10	100.00
1045.2	53.36	0.91	21.47	7.99	0.18	3.09	8.56	3.54	0.79	0.11	100.00
1035.2	53.50	0.88	21.87	8.02	0.18	2.80	8.22	3.63	0.80	0.11	100.00
1025.2	53.69	0.80	22.21	8.04	0.19	2.55	7.87	3.72	0.82	0.11	100.00
1015.2	53.92	0.71	22.51	8.07	0.19	2.32	7.53	3.81	0.85	0.11	100.00
1005.2	54.12	0.63	22.82	8.07	0.19	2.09	7.20	3.89	0.87	0.12	100.00
995.2	54.31	0.56	23.10	8.07	0.20	1.89	6.90	3.97	0.88	0.12	100.00
985.2	54.49	0.50	23.37	8.06	0.20	1.70	6.62	4.04	0.90	0.12	100.00
975.2	54.66	0.44	23.63	8.04	0.20	1.53	6.35	4.11	0.92	0.12	100.00
965.2	54.82	0.39	23.88	8.01	0.22	1.36	6.10	4.18	0.93	0.12	100.00
955.2	55.03	0.36	23.94	8.09	0.22	1.25	5.76	4.26	0.95	0.13	100.00
945.2	55.74	0.34	23.88	7.68	0.23	1.03	5.53	4.45	1.00	0.13	100.00
935.2	56.34	0.32	23.80	7.37	0.24	0.87	5.27	4.61	1.05	0.14	100.00
925.2	56.95	0.30	23.72	7.06	0.25	0.72	5.02	4.76	1.08	0.14	100.00
915.2	57.53	0.27	23.62	6.76	0.26	0.59	4.77	4.91	1.13	0.15	100.00
905.2	58.10	0.26	23.53	6.45	0.26	0.48	4.53	5.06	1.17	0.15	100.00
895.2	58.63	0.25	23.43	6.16	0.28	0.39	4.29	5.19	1.21	0.17	100.00
885.2	59.16	0.24	23.35	5.87	0.29	0.30	4.05	5.32	1.25	0.17	100.00
875.2	59.68	0.23	23.25	5.58	0.30	0.23	3.82	5.45	1.29	0.17	100.00
865.2	60.17	0.22	23.15	5.31	0.30	0.18	3.60	5.57	1.33	0.18	100.00
855.2	60.65	0.22	23.05	5.04	0.31	0.12	3.37	5.69	1.36	0.18	100.00

845.2	61.12	0.19	22.95	4.78	0.32	0.09	3.16	5.79	1.40	0.19	100.00
835.2	61.59	0.18	22.85	4.51	0.34	0.06	2.94	5.89	1.45	0.19	100.00
825.2	62.05	0.16	22.76	4.26	0.34	0.03	2.74	5.98	1.49	0.20	100.00
815.2	62.50	0.15	22.65	4.01	0.35	0.02	2.52	6.06	1.53	0.20	100.00
805.2	62.99	0.12	22.52	3.77	0.36	0.01	2.28	6.15	1.59	0.22	100.00
795.2	63.46	0.11	22.41	3.53	0.39	0.00	2.03	6.22	1.65	0.22	100.00
785.2	63.92	0.10	22.30	3.27	0.40	0.00	1.81	6.27	1.70	0.23	100.00
775.2	64.42	0.09	22.20	2.98	0.41	0.00	1.58	6.32	1.76	0.24	100.00
765.2	65.03	0.09	22.08	2.63	0.44	0.00	1.39	6.22	1.87	0.25	100.00
755.2	66.31	0.09	21.74	2.15	0.50	0.00	1.35	5.46	2.12	0.29	100.00
745.2	67.40	0.10	21.44	1.77	0.55	0.00	1.30	4.79	2.33	0.33	100.00
735.2	68.33	0.10	21.19	1.45	0.61	0.00	1.26	4.19	2.52	0.35	100.00
725.2	69.15	0.10	20.96	1.19	0.65	0.00	1.22	3.66	2.69	0.38	100.00
715.2	69.84	0.10	20.77	0.97	0.68	0.00	1.19	3.19	2.85	0.40	100.00
705.2	68.98	0.11	21.80	0.77	0.79	0.00	1.20	2.62	3.28	0.46	100.00
695.2	68.15	0.11	22.74	0.61	0.88	0.00	1.21	2.16	3.64	0.51	100.00
685.2	67.27	0.11	23.21	0.49	1.07	0.00	1.31	1.80	4.10	0.63	100.00
675.2	45.87	0.04	24.50	0.91	10.31	0.00	7.83	2.96	1.55	6.03	100.00
665.2	39.63	0.03	23.03	0.81	14.10	0.00	10.44	2.62	1.09	8.25	100.00
655.2	35.95	0.03	21.77	0.69	16.56	0.00	12.14	2.34	0.84	9.68	100.00

S4. Model BHFC2: BH150, 5 wt% H₂O, FMQ +1, 0.3 GPa

T (°C)	Model BHFC2 – Normalized liquid composition (wt%)										
	SiO ₂	TiO ₂	Al ₂ O ₃	FeO _t	MnO	MgO	CaO	Na ₂ O	K ₂ O	P ₂ O ₅	Total
967.38	66.39	0.62	16.88	3.67	0.06	1.41	4.60	3.98	2.18	0.21	100.00
957.38	66.52	0.62	16.96	3.54	0.06	1.32	4.58	4.00	2.19	0.21	100.00
947.38	66.83	0.59	17.10	3.31	0.07	1.19	4.42	4.05	2.21	0.22	100.00
937.38	67.14	0.57	17.24	3.08	0.07	1.06	4.28	4.09	2.24	0.22	100.00
927.38	67.43	0.54	17.36	2.89	0.07	0.96	4.13	4.13	2.27	0.22	100.00
917.38	67.69	0.52	17.48	2.70	0.07	0.86	4.00	4.17	2.29	0.22	100.00
907.38	68.20	0.50	17.33	2.51	0.07	0.83	3.79	4.18	2.34	0.23	100.00
897.38	68.71	0.48	17.18	2.34	0.07	0.80	3.60	4.19	2.40	0.23	100.00
887.38	69.19	0.47	17.03	2.19	0.07	0.77	3.41	4.18	2.45	0.24	100.00
877.38	69.65	0.46	16.84	2.05	0.07	0.73	3.26	4.18	2.51	0.24	100.00
867.38	70.13	0.44	16.67	1.91	0.08	0.68	3.10	4.17	2.57	0.25	100.00
857.38	70.59	0.41	16.49	1.78	0.09	0.64	2.97	4.15	2.63	0.26	100.00
847.38	71.05	0.38	16.30	1.68	0.09	0.59	2.83	4.12	2.69	0.27	100.00
837.38	71.50	0.35	16.11	1.59	0.09	0.54	2.70	4.09	2.75	0.28	100.00
827.38	71.92	0.33	15.93	1.49	0.09	0.51	2.57	4.06	2.82	0.28	100.00
817.38	72.35	0.30	15.75	1.40	0.09	0.47	2.46	4.02	2.88	0.29	100.00
807.38	72.76	0.28	15.56	1.32	0.10	0.44	2.35	3.97	2.93	0.29	100.00
797.38	73.16	0.26	15.38	1.23	0.10	0.41	2.23	3.93	3.00	0.30	100.00
787.38	73.56	0.24	15.20	1.16	0.10	0.38	2.13	3.87	3.06	0.31	100.00
777.38	73.96	0.22	15.03	1.09	0.10	0.34	2.02	3.81	3.12	0.31	100.00
767.38	74.32	0.20	14.84	1.03	0.10	0.32	1.93	3.75	3.19	0.32	100.00
757.38	74.98	0.19	14.50	0.94	0.11	0.29	1.78	3.61	3.27	0.33	100.00
747.38	74.66	0.18	14.77	0.82	0.13	0.21	1.54	3.44	3.84	0.41	100.00
737.38	74.08	0.17	15.20	0.70	0.15	0.16	1.36	3.16	4.52	0.49	100.00
727.38	73.10	0.17	15.97	0.60	0.20	0.13	1.34	2.75	5.07	0.66	100.00
717.38	71.23	0.16	17.66	0.55	0.32	0.12	1.65	2.26	5.02	1.04	100.00
707.38	69.70	0.16	19.01	0.50	0.41	0.11	1.96	1.81	5.02	1.33	100.00
697.38	68.37	0.15	20.19	0.45	0.48	0.10	2.22	1.48	4.99	1.57	100.00
687.38	67.16	0.14	21.27	0.42	0.55	0.09	2.45	1.22	4.92	1.79	100.00
677.38	62.64	0.12	20.87	0.44	1.50	0.09	4.94	1.07	4.49	3.84	100.00
667.38	7.51	0.03	1.81	0.15	13.41	0.08	41.83	0.00	0.17	35.01	100.00
657.38	7.51	0.03	1.81	0.15	13.41	0.08	41.83	0.00	0.17	35.01	100.00

S5. Model BNFC5a: BN14, 5 wt% H₂O, FMQ -1, 0.3 GPa

T (°C)	Model BNFC5 – Normalized liquid composition (wt%)										
	SiO ₂	TiO ₂	Al ₂ O ₃	FeOt	MnO	MgO	CaO	Na ₂ O	K ₂ O	P ₂ O ₅	Total
988.28	66.40	0.37	16.41	3.33	0.09	1.38	4.14	3.44	4.27	0.17	100.00
978.28	66.46	0.37	16.48	3.26	0.09	1.27	4.15	3.46	4.28	0.17	100.00
968.28	66.52	0.37	16.54	3.19	0.09	1.17	4.16	3.47	4.30	0.18	100.00
958.28	66.57	0.37	16.61	3.11	0.09	1.07	4.18	3.49	4.32	0.18	100.00
948.28	66.66	0.37	16.69	3.05	0.09	0.98	4.14	3.50	4.35	0.18	100.00
938.28	66.79	0.37	16.80	2.99	0.09	0.87	3.99	3.54	4.38	0.18	100.00
928.28	66.92	0.37	16.91	2.93	0.09	0.77	3.85	3.56	4.42	0.18	100.00
918.28	67.04	0.37	17.00	2.87	0.09	0.68	3.73	3.58	4.46	0.18	100.00
908.28	67.17	0.36	17.11	2.80	0.09	0.59	3.60	3.60	4.49	0.18	100.00
898.28	67.30	0.36	17.18	2.74	0.09	0.52	3.48	3.64	4.51	0.18	100.00
888.28	67.41	0.36	17.27	2.68	0.09	0.44	3.36	3.65	4.55	0.18	100.00
878.28	67.58	0.35	17.27	2.63	0.09	0.39	3.23	3.66	4.60	0.19	100.00
868.28	67.85	0.35	17.14	2.63	0.11	0.36	3.04	3.65	4.68	0.19	100.00
858.28	68.11	0.36	17.01	2.63	0.11	0.33	2.86	3.64	4.77	0.19	100.00
848.28	68.39	0.35	16.88	2.63	0.11	0.31	2.69	3.61	4.85	0.20	100.00
838.28	68.75	0.34	16.75	2.50	0.11	0.24	2.55	3.59	4.96	0.20	100.00
828.28	69.14	0.29	16.60	2.39	0.11	0.20	2.43	3.56	5.07	0.21	100.00
818.28	69.50	0.27	16.44	2.30	0.11	0.17	2.31	3.52	5.18	0.21	100.00
808.28	69.84	0.23	16.30	2.21	0.12	0.14	2.19	3.47	5.29	0.21	100.00
798.28	70.15	0.21	16.15	2.13	0.12	0.12	2.09	3.42	5.39	0.22	100.00
788.28	70.48	0.19	16.00	2.04	0.12	0.10	1.98	3.36	5.51	0.22	100.00
778.28	70.79	0.18	15.86	1.95	0.12	0.07	1.88	3.30	5.61	0.24	100.00
768.28	71.10	0.16	15.71	1.85	0.13	0.05	1.80	3.24	5.73	0.24	100.00
758.28	71.40	0.15	15.57	1.76	0.13	0.04	1.70	3.17	5.83	0.25	100.00
748.28	72.63	0.14	14.95	1.58	0.14	0.03	1.62	3.06	5.58	0.27	100.00
738.28	73.74	0.13	14.37	1.44	0.16	0.02	1.54	2.92	5.37	0.30	100.00
728.28	72.96	0.12	14.85	1.31	0.39	0.00	1.83	2.60	5.19	0.75	100.00
718.28	70.40	0.12	16.35	1.10	0.78	0.00	2.50	2.17	5.05	1.52	100.00
708.28	68.27	0.12	17.63	0.91	1.10	0.00	3.09	1.85	4.89	2.15	100.00
698.28	66.34	0.11	18.81	0.75	1.37	0.00	3.63	1.61	4.71	2.68	100.00
688.28	64.48	0.11	19.92	0.62	1.62	0.00	4.15	1.41	4.51	3.18	100.00
678.28	62.69	0.11	20.98	0.51	1.85	0.00	4.67	1.18	4.38	3.63	100.00
668.28	10.10	0.02	3.34	0.18	16.22	0.00	37.96	0.03	0.20	31.95	100.00
658.28	9.89	0.02	3.11	0.16	16.30	0.00	38.18	0.03	0.18	32.13	100.00

S6. Model BNFC5b: BN12-1, 5 wt% H₂O, FMQ -3, 0.3 GPa

T (°C)	Model BNFC5 – Normalized liquid composition (wt%)										
	SiO ₂	TiO ₂	Al ₂ O ₃	FeO _t	MnO	MgO	CaO	Na ₂ O	K ₂ O	P ₂ O ₅	Total
1004.88	67.25	0.35	15.78	3.35	0.09	1.50	3.99	3.11	4.40	0.17	100.00
994.88	67.31	0.35	15.84	3.28	0.09	1.39	4.02	3.12	4.43	0.18	100.00
984.88	67.37	0.35	15.91	3.21	0.09	1.28	4.03	3.13	4.45	0.18	100.00
974.88	67.43	0.35	15.97	3.14	0.09	1.18	4.04	3.15	4.47	0.18	100.00
964.88	67.50	0.35	16.04	3.05	0.09	1.08	4.04	3.17	4.49	0.18	100.00
954.88	67.55	0.36	16.10	2.98	0.09	1.00	4.05	3.18	4.51	0.18	100.00
944.88	67.61	0.36	16.16	2.91	0.09	0.92	4.06	3.19	4.52	0.18	100.00
934.88	67.67	0.36	16.22	2.84	0.09	0.83	4.05	3.21	4.55	0.18	100.00
924.88	67.80	0.36	16.32	2.78	0.09	0.73	3.93	3.23	4.58	0.18	100.00
914.88	67.91	0.36	16.42	2.72	0.09	0.64	3.80	3.25	4.61	0.18	100.00
904.88	68.04	0.35	16.51	2.66	0.09	0.56	3.69	3.27	4.65	0.18	100.00
894.88	68.16	0.35	16.59	2.60	0.09	0.48	3.57	3.29	4.68	0.18	100.00
884.88	68.28	0.35	16.67	2.53	0.09	0.41	3.47	3.31	4.70	0.18	100.00
874.88	68.38	0.35	16.75	2.47	0.09	0.35	3.36	3.32	4.74	0.19	100.00
864.88	68.56	0.34	16.73	2.43	0.09	0.31	3.23	3.33	4.79	0.19	100.00
854.88	68.83	0.35	16.60	2.42	0.11	0.27	3.04	3.32	4.87	0.19	100.00
844.88	69.11	0.35	16.46	2.42	0.11	0.24	2.88	3.29	4.96	0.19	100.00
834.88	69.42	0.33	16.32	2.40	0.11	0.22	2.70	3.27	5.04	0.20	100.00
824.88	69.79	0.32	16.19	2.27	0.11	0.17	2.58	3.23	5.15	0.20	100.00
814.88	70.18	0.28	16.03	2.16	0.11	0.14	2.45	3.20	5.25	0.21	100.00
804.88	70.51	0.24	15.87	2.08	0.12	0.12	2.34	3.15	5.37	0.21	100.00
794.88	70.86	0.22	15.72	1.97	0.12	0.10	2.23	3.10	5.47	0.21	100.00
784.88	71.19	0.20	15.56	1.88	0.12	0.07	2.13	3.05	5.57	0.22	100.00
774.88	71.50	0.19	15.41	1.79	0.12	0.05	2.04	2.99	5.68	0.22	100.00
764.88	71.84	0.17	15.26	1.67	0.12	0.04	1.94	2.93	5.79	0.24	100.00
754.88	72.28	0.16	15.08	1.45	0.13	0.03	1.84	2.89	5.90	0.24	100.00
744.88	73.36	0.15	14.52	1.32	0.14	0.02	1.76	2.78	5.69	0.26	100.00
734.88	74.43	0.14	13.95	1.21	0.15	0.01	1.70	2.65	5.48	0.29	100.00
724.88	71.79	0.13	15.16	1.04	0.63	0.00	2.50	2.16	5.34	1.24	100.00
714.88	69.32	0.13	16.52	0.87	1.08	0.00	3.14	1.79	5.18	1.96	100.00
704.88	67.42	0.13	17.87	0.72	1.46	0.00	3.49	1.53	4.99	2.39	100.00
694.88	65.47	0.12	19.02	0.61	1.80	0.00	4.00	1.32	4.78	2.89	100.00

684.88	63.45	0.12	20.11	0.50	2.10	0.00	4.59	1.15	4.55	3.44	100.00
674.88	60.67	0.11	21.08	0.44	2.63	0.00	5.56	1.00	4.23	4.29	100.00
664.88	12.80	0.02	5.63	0.21	17.60	0.00	34.43	0.09	0.29	28.94	100.00
654.88	12.39	0.02	5.22	0.18	17.80	0.00	34.82	0.08	0.24	29.25	100.00

S7. Model BNFC3: BN14, 5 wt% H₂O, FMQ -1, 0.25 GPa

T (°C)	Model BNFC3 – Normalized liquid composition (wt%)										
	SiO ₂	TiO ₂	Al ₂ O ₃	FeO _t	MnO	MgO	CaO	Na ₂ O	K ₂ O	P ₂ O ₅	Total
	66.40	0.37	16.41	3.33	0.09	1.38	4.14	3.44	4.27	0.17	100.00
970.27	66.45	0.37	16.48	3.26	0.09	1.27	4.16	3.46	4.28	0.17	100.00
960.27	66.51	0.37	16.55	3.18	0.09	1.17	4.17	3.47	4.30	0.18	100.00
950.27	66.57	0.37	16.61	3.11	0.09	1.07	4.18	3.49	4.32	0.18	100.00
940.27	66.67	0.37	16.70	3.05	0.09	0.98	4.11	3.50	4.35	0.18	100.00
930.27	66.79	0.37	16.81	2.99	0.09	0.87	3.97	3.54	4.39	0.18	100.00
920.27	66.93	0.37	16.91	2.93	0.09	0.77	3.83	3.56	4.42	0.18	100.00
910.27	67.06	0.37	17.01	2.87	0.09	0.67	3.70	3.59	4.46	0.18	100.00
900.27	67.18	0.36	17.11	2.80	0.09	0.59	3.57	3.61	4.49	0.18	100.00
890.27	67.30	0.36	17.19	2.74	0.09	0.52	3.46	3.64	4.52	0.18	100.00
880.27	67.43	0.35	17.29	2.68	0.09	0.44	3.33	3.66	4.55	0.18	100.00
870.27	67.69	0.35	17.16	2.67	0.09	0.41	3.15	3.65	4.63	0.19	100.00
860.27	67.95	0.36	17.03	2.66	0.11	0.38	2.97	3.63	4.71	0.19	100.00
850.27	68.23	0.36	16.90	2.67	0.11	0.35	2.78	3.62	4.80	0.19	100.00
840.27	68.55	0.31	16.77	2.63	0.11	0.32	2.63	3.60	4.89	0.20	100.00
830.27	68.99	0.29	16.65	2.44	0.11	0.23	2.49	3.57	5.02	0.20	100.00
820.27	69.32	0.27	16.50	2.35	0.11	0.20	2.37	3.55	5.13	0.21	100.00
810.27	69.68	0.23	16.35	2.26	0.12	0.17	2.25	3.50	5.23	0.21	100.00
800.27	70.00	0.21	16.20	2.17	0.12	0.14	2.14	3.46	5.35	0.22	100.00
790.27	70.44	0.19	15.99	2.06	0.12	0.11	1.99	3.39	5.49	0.22	100.00
780.27	70.96	0.18	15.70	1.94	0.13	0.09	1.82	3.27	5.68	0.23	100.00
770.27	71.50	0.17	15.42	1.82	0.13	0.05	1.65	3.13	5.89	0.24	100.00
760.27	72.42	0.15	14.96	1.72	0.14	0.03	1.56	2.96	5.79	0.27	100.00
750.27	73.43	0.14	14.46	1.61	0.16	0.02	1.51	2.78	5.59	0.30	100.00
740.27	74.59	0.15	14.00	1.27	0.16	0.01	1.45	2.59	5.46	0.33	100.00
730.27	72.37	0.14	15.82	1.11	0.35	0.00	1.90	1.88	5.53	0.91	100.00

S8. Crystallization Phases

Model PAFC7: PA118, 5 wt% H₂O, FMQ -1, 3500bar		
T(°C)	Phases	Melt (%)
939	Liquid	100
938	Liquid + Opx	99.74
798	Liquid + (Opx) + Flds	96.16
768	Liquid + (Opx + Flds) + Rhm-oxide	86.23
758	Liquid + (Opx + Flds + Rhm-oxide) + Qtz	82.64
718	Liquid + (Opx + Flds + Rhm-oxide + Qtz) + Garnet + Leucite	2.74
678	Liquid + (Opx + Flds + Rhm-oxide + Qtz + Garnet + Leucite) + Muscovite + Sillimanite	0.31

Model CDFC4: CD155, 5 wt% H₂O, FMQ -3, 4000bar		
T(°C)	Phases	Melt (%)
1176	Liquid	100
1175	Liquid + Ol	99.73
1105	Liquid + (Ol) + Cpx	94.35
955	Liquid + (Ol + Cpx) + Flds	65.69
945	Liquid + (Ol + Cpx + Flds) + Garnet	68.82
845	Liquid + (Ol + Cpx + Flds + Garnet) + Rhm-oxide	45.91
765	Liquid + (Ol + Cpx + Flds + Garnet + Rhm-oxide) + Leucite	34.27
715	Liquid + (Ol + Cpx + Flds + Garnet + Rhm-oxide + Leucite) + Qtz	21.49
685	Liquid + (Ol + Cpx + Flds + Garnet + Rhm-oxide + Leucite + Qtz) + Muscovite + Sillimanite	13.55

Model BHFC2: BH150, 5 wt% H₂O, FMQ +1, 0.3 GPa		
T(°C)	Phases	Melt (%)
968	Liquid	100
967	Liquid + Opx	100
957	Liquid + (Opx) + Cpx + Spi	99.42
917	Liquid + (Opx + Cpx + Spi) + Flds	95.36
857	Liquid + (Opx + Cpx + Spi + Flds) + Rhm-oxide	82.8
757	Liquid + (Opx + Cpx + Spi + Flds + Rhm-oxide) + Bt	65.2
747	Liquid + (Opx + Cpx + Spi + Flds + Rhm-oxide + Bt) + Qtz	53.77
707	Liquid + (Opx + Cpx + Spi + Flds + Rhm-oxide + Bt + Qtz) + Leucite	16.23
677	Liquid + (Opx + Cpx + Spi + Flds + Rhm-oxide + Bt + Qtz + Leucite) + Sillimanite + Ap	4.35
667	Liquid + (Opx + Cpx + Spi + Flds + Rhm-oxide + Bt + Qtz + Leucite + Sillimanite + Ap) + Garnet + Muscovite + Corundum	0.49

Model BNFC5a: BN14, 5 wt% H₂O, FMQ -1, 0.3 GPa		
T(°C)	Phases	Melt (%)
989	Liquid	100
988	Liquid + Opx	99.65
948	Liquid + (Opx) + Cpx	97.87
878	Liquid + (Opx + Cpx) + Flds	92.76
828	Liquid + (Opx + Cpx + Flds) + Rhm-oxide	83.8
748	Liquid + (Opx + Cpx + Flds + Rhm-oxide) + Garnet	64.34
728	Liquid + (Opx + Cpx + Flds + Rhm-oxide + Garnet) + Qtz	23.39
688	Liquid + (Opx + Cpx + Flds + Rhm-oxide + Garnet + Qtz) + Leucite	5.57
668	Liquid + (Opx + Cpx + Flds + Rhm-oxide + Garnet + Qtz + Leucite) + Muscovite + Sillimanite	0.57

Model BNFC5b: BN12-1, 5 wt% H₂O, FMQ -3, 0.3 GPa		
T(°C)	Phases	Melt (%)
1006	Liquid	100
1005	Liquid + Opx	99.71
935	Liquid + (Opx) + Cpx	96.82
865	Liquid + (Opx + Cpx) + Flds	92.17
815	Liquid + (Opx + Cpx + Flds) + Rhm-oxide	83.69
755	Liquid + (Opx + Cpx + Flds + Rhm-oxide) + Garnet	74.11
725	Liquid + (Opx + Cpx + Flds + Rhm-oxide + Garnet) + Qtz	14.15
715	Liquid + (Opx + Cpx + Flds + Rhm-oxide + Garnet + Qtz) + Ap	8.3
675	Liquid + (Opx + Cpx + Flds + Rhm-oxide + Garnet + Qtz + Ap) + Sillimanite	3.45
665	Liquid + (Opx + Cpx + Flds + Rhm-oxide + Garnet + Qtz + Ap + Sillimanite) + Muscovite + Leucite	0.54

Model BNFC3: BN14, 5 wt% H₂O, FMQ -1, 0.25 GPa		
T(°C)	Phases	Melt (%)
990	Liquid	100
980	Liquid + Opx	99.6
940	Liquid + (Opx) + Cpx	97.8
870	Liquid + (Opx + Cpx) + Flds	92
840	Liquid + (Opx + Cpx + Flds) + Rhm-oxide	87
740	Liquid + (Opx + Cpx + Flds + Rhm-oxide) + Ol	53
730	Liquid + (Opx + Cpx + Flds + Rhm-oxide + Ol) + Qtz	19